

# Numerical modeling of the behavior of concrete exposed to chloride ions by coupling age and mechanical stresses

Article Info:

Article history: Received 2024-01-03 / Accepted 2024-05-13 / Available online 2024-05-13

doi: 10.18540/jcecv110iss3pp18577



**Bendjaiche Roubila**

ORCID: <https://orcid.org/0000-0003-1025-4832>

Laboratory of Civil Engineering and Hydraulics, University of 8 Mai 1945 - Guelma, Algeria

E-mail: [bendjaiche.roubila@univ-guelma.dz](mailto:bendjaiche.roubila@univ-guelma.dz)

**Boudjehm Hocine**

ORCID: <https://orcid.org/0000-0003-0086-8355>

Laboratory of Civil Engineering and Hydraulics, University of 8 Mai 1945 - Guelma, Algeria

E-mail: [boudjehm.hocine@univ-guelma.dz](mailto:boudjehm.hocine@univ-guelma.dz)

**Nafa Zahreddine**

ORCID: <https://orcid.org/0000-0003-2187-6426>

Laboratory of Civil Engineering and Hydraulics, University of 8 Mai 1945 - Guelma, Algeria

E-mail: [nafa.zahreddine@univ-guelma.dz](mailto:nafa.zahreddine@univ-guelma.dz)

**Bouteldja Fathe**

ORCID: <https://orcid.org/0000-0003-0958-6928>

Laboratory of Civil Engineering and Hydraulics, University of 8 Mai 1945 - Guelma, Algeria

E-mail: [bouteldja.fathe@univ-guelma.dz](mailto:bouteldja.fathe@univ-guelma.dz)

## Abstract

This study proposes a quantitative examination of the issue of chloride ion infiltration in concrete under mechanical strain in a hostile setting while considering the influence of time, commonly referred to as the aging effect. The relationship between the diffusion coefficient and age, when subjected to specific levels of uniaxial or biaxial stresses for various W/C ratios, has allowed us to assess the concentration of chloride ions and the time needed for corrosion to begin through the coating layer in three dimensions. The numerical model results corroborate the notion that the corrosion process is affected by the fluctuation of the diffusion coefficient, which is directly linked to the age factor and the mechanical stresses exerted on the concrete. The model also emphasizes the extended distribution of chloride ion concentration at a certain depth, which is connected to the ratio of water to cement, influenced by the diffusion coefficient and the degree of mechanical stress in older structures.

**Keywords:** Modeling. Coupling. Uniaxial and biaxial stresses. Aging. Chloride ions. Diffusion coefficient.

## 1. Introduction

The durability of reinforced concrete structures depends on their ability to withstand aggressive factors, particularly chloride ion attacks, by means of the protective properties of their constituent materials. Corrosion is influenced by various complex factors that arise from the physical and/or chemical interaction between the material and its environment. These factors include aggressiveness, age, cracking, the water/cement ratio, and the level of stress within the cementitious matrix. All of these factors are of significant importance. Reinforced concrete structures are engineered for long-term durability [1], but they gradually deteriorate due to corrosion induced by the harsh environmental conditions they encounter [2], [3]. The steel, which is initially shielded by the concrete coating, can lose its protective properties due to either carbonation caused

by carbon dioxide or the infiltration of chloride ions from seawater, sea spray, or de-icing salts [4]. This phenomenon poses a greater risk when the structure is exposed to mechanical strain [5] and deteriorates progressively [6], [7]. The interplay between stress levels and age contributes to a fluctuation in the diffusion coefficient, thereby expediting the progression of mechanical or physico-chemical pathology that can impact concrete.

The lifespan of a reinforced concrete structure can be divided into two distinct periods [8]: an initial period, determined by the rate at which the concrete coating is neutralized, and a subsequent period, characterized by the corrosion of the reinforcement and eventual deterioration of the structure. To accurately determine the lifespan of structures, it is best to utilize dependable and efficient models that depict the progression of chloride ions and establish the duration needed for the reinforcement to lose its protective layer. There are two types of penetration, depending on the characteristics of the medium [9]. In an environment that is already filled, such as structures that are exposed to seawater, chloride ions enter the structure through the process of diffusion, which occurs due to a difference in concentration and increases the likelihood of corrosion starting. Within tidal zones, where there is a cyclic humidification-drying environment, the process of capillary absorption is succeeded by diffusion in saturated areas [4].

The objective of this study is to develop a precise numerical model that describes the phenomenon of ion propagation, considering both the stress level [5] and the aging effect [10]. The model will enable the determination of multiple quantities, including concentration, corrosion initiation time, thickness, and stress level, as well as the generation of a three-dimensional representation. The constructed model will validate its reliability by describing the relationship between concentration, coating thickness, and corrosion initiation time.

## 2. Model basics

The majority of models that describe the infiltration of chloride ions in concrete are based on Fick's second law widely used [8] and [9].

$$\frac{\partial C(x,t)}{\partial t} = D_c \frac{\partial^2 C(x,t)}{\partial x^2} \quad (1)$$

where  $C(x,t)$  is the concentration of chloride ions at a depth  $x$  and a time  $t$ ,  $D_c$  is the effective diffusion coefficient of chloride ions, [ $m^2/s$ ].

Theoretically, Eq. (1) is a partial differential Eq. without an analytical solution. It can be obtained by assuming that the diffusion of chloride ions in concrete is a one-dimensional semi-infinite medium with constant surface chloride concentrations. If we assume that the initial chloride concentration in the concrete is zero, a solution of the error function of Eq. (1) can be obtained as:

$$C(x,t) = C_s \left[ 1 - \text{ERF} \left( \frac{x}{2\sqrt{D_c t}} \right) \right] \quad (2)$$

where  $C_s$  is the concentration of chloride ions at the surface, [%], and  $x$  is the coating depth, [mm].

The diffusion coefficient changes over time as a result of concrete maturation. Thus, older concrete is more susceptible to chloride penetration. Eq. (3) is used to determine the nominal value of the time-dependent diffusion coefficient. Its evolution over time can be predicted using reference values and the aging coefficient developed by Lehner and Konecny in 2017 [10], reformulated by Zhao *et al.* in 2020 [11], and Hornakova *et al.* in 2020 [12]. Taking age into consideration, we note:

$$D_0 = D_{c,ref} \left( \frac{T_{ref}}{T} \right)^M \quad (3)$$

where  $D_{c,ref}$  is the reference diffusion coefficient for chloride ions, [ $m^2/s$ ],  $D_0$  is the initial diffusion coefficient of chloride ions without stresses, [ $m^2/s$ ],  $T$  is the chloride exposure time, [s],  $T_{ref}$  is the measured reference time, [s], and  $M$  is the age factor.

### 3. Experimental data

#### 3.1 Concrete compression

In 2020, X. Cheng *et al.* [5] conducted experiments to study the diffusion law of chloride ions in concrete under compressive stress [5]. The specimens were created with Portland cement, which has a characteristic compressive strength of 42.5 MPa. Gravel with a maximum size of 20 mm and a density of 1550 kg/m<sup>3</sup> is used for coarse aggregate. Natural river sand is used as fine aggregate with a fineness modulus of 2 to 3. All concrete specimens were produced using a polycarboxylic ether superplasticizer. The concrete specimens are then carefully placed in the loading device's uniaxial or biaxial direction, with X-pressure readings used to monitor and control compressive stress [5]. The concrete samples were divided into three categories based on compressive stresses of 47.21 MPa, 52.68 MPa, and 56.78 MPa, respectively. The uniaxial and biaxial cases had water/cement (W/C) ratios of 0.44, 0.4, and 0.36, respectively. The following formula calculates stress levels:

$$\mu_{1,2} = \frac{\sigma_{c(x,y)}}{F_c} \quad (4)$$

where  $\mu_{1,2}$  represents stress levels index 1 for uniaxial and 2 for biaxial,  $\sigma_{c(x,y)}$  is the mechanical compressive stress applied in both directions, [MPa],  $F_c$  and the compressive strength measured at 28 days.

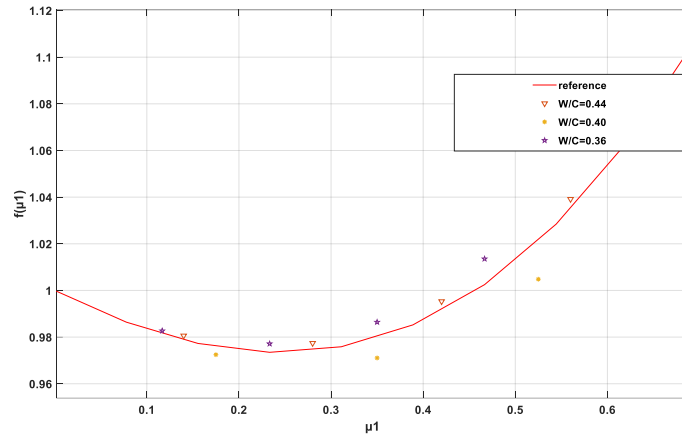
#### 3.2 Diffusion of chloride ions

According to Hornakova *et al.* [12], the chloride ion penetration experiment was carried out in an artificial climate simulation box with a temperature range of 20° to 22°C. The concrete specimens were exposed to chloride salts for two months. To minimize the impact of errors, three values were chosen for the drilling depth of the same layer. Following this, the chloride ion concentration of the concrete powder sample was determined. The model for the apparent chloride ion diffusion coefficient under a sustained uniaxial stress level proposed by X Cheng *et al.* [5] is as follows:

$$D_c(\mu_1) = D_0(1 - 0.2\mu_1 + 0.3\mu_1^2 + 0.3\mu_1^3) \quad (5)$$

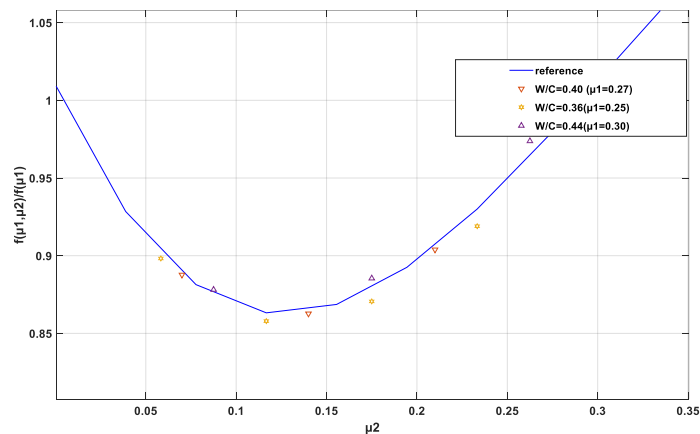
where  $D_0$  is the initial unstressed chloride ion diffusion coefficient, [m<sup>2</sup>/s], and  $D_c$  is the chloride ion diffusion coefficient with stresses, [m<sup>2</sup>/s].

Figure 1 shows the relationship between stress level  $\mu_1$  and the uniaxial stress function  $f(\mu_1)$  for different ratios (W/C) 0.40, 0.36, 0.44, presented by Cheng *et al.* [5] which is approximately a cubic curve.



**Figure 1 - Relationship between stress level  $\mu_1$  and uniaxial stress function  $f(\mu_1)$  for different ratios W/C**

Concrete’s chloride ion diffusion capacity is affected by both  $\mu_1$  and  $\mu_2$  under biaxial compressive loading. Figure 2 demonstrated by Cheng *et al.* [5] illustrates the relationship between stress level  $\mu_2$  and the stress function  $(\mu_1, \mu_2)$ , where  $\mu_1$  remains constant for each (W/C) ratio of 0.44, 0.40, and 0.36.



**Figure 2 - Relationship between stress level  $\mu_2$  and stress function  $f(\mu_1, \mu_2)$  with held ( $\mu_1$ ) constant for each ratio W/C**

The model of the apparent chloride ion diffusion coefficient under a sustained biaxial stress level continued proposed by Cheng *et al.* [5] can also be obtained as follows:

$$Dc(\mu_1, \mu_2) = D_0(1.01 - 2.39\mu_2 + 12.59\mu_2^2 - 14.36\mu_2^3)(1 - 0.2\mu_1 + 0.3\mu_1^2 + 0.3\mu_1^3) \quad (6)$$

Development of the equations required for modeling in Matlab R2021a and the Gauss integral using polar coordinates and the Jacobian gave us the following relationships:

\*Uni-axial stress case:

$$\frac{\alpha(x,t)^2}{c_s^2} = \left[ 1 - e^{\frac{-x^2}{2Dc(\mu_1)t^{(m-1)}} / (m-1)} \right] \quad (7)$$

\* Bi-axial stress case:

$$\frac{C(x,t)^2}{C_s^2} = \left[ 1 - e^{-\frac{x^2}{2D_c(\mu_1, \mu_2)t^{(m-1)/(m-1)}}} \right] \quad (8)$$

The values calculated by the above equations for a surface concentration  $C_s$  is 0.20%, proposed by Lehner *et al.* [10], an age factor  $M=0.284$  for ordinary concrete [10] and a reference diffusion coefficient equal to give chloride ion  $D_{c,ref} = 5.585 \times 10^{-12}$  (m<sup>2</sup>/s) [10]. The values calculated by our model are represented in Tables 1, 2 and 3:

**Table 1- Chloride ion diffusion coefficients values W/C=0.44 and Fc=47.21 MPa**

Uniaxial stress				Biaxial stress				
Sample	$\sigma_{c(x)}$ (MPa)	$\mu_1$	Dc( $\mu_1$ ) (m <sup>2</sup> /s)	Sample	$\sigma_{c(x)}$ (MPa)	$\sigma_{c(y)}$ (MPa)	$\mu_2$ $\mu_1 = 0.3$	Dc( $\mu_1$ ) (m <sup>2</sup> /s)
1	7.08	0.15	$7.55 \times 10^{-12}$	1	14.16	3.54	0.07	$6.72 \times 10^{-12}$
2	14.16	0.30	$7.47 \times 10^{-12}$	2	14.16	7.08	0.15	$6.52 \times 10^{-12}$
3	21.24	0.45	$7.66 \times 10^{-12}$	3	14.16	10.63	0.22	$7.16 \times 10^{-12}$
4	28.33	0.60	$8.07 \times 10^{-12}$	4	14.16	14.16	0.30	$7.67 \times 10^{-12}$
$D_0 = 7.65 \times 10^{-12} \left( \frac{m^2}{s} \right)$				$D_0 = 7.65 \times 10^{-12} \left( \frac{m^2}{s} \right)$				

**Table 2 - Chloride ion diffusion coefficients value W/C=0.40 and Fc=52.68 MPa**

Uniaxial stress				Biaxial stress				
Sample	$\sigma_{c(x)}$ (MPa)	$\mu_1$	Dc( $\mu_1$ ) (m <sup>2</sup> /s)	Sample	$\sigma_{c(x)}$ (MPa)	$\sigma_{c(y)}$ (MPa)	$\mu_2$ $\mu_1 = 0.3$	Dc( $\mu_1$ ) (m <sup>2</sup> /s)
1	7.08	0.13	$6.10 \times 10^{-12}$	1	14.16	3.54	0.06	$5.44 \times 10^{-12}$
2	14.16	0.25	$5.98 \times 10^{-12}$	2	14.16	7.08	0.13	$5.14 \times 10^{-12}$
3	21.24	0.27	$6.16 \times 10^{-12}$	3	14.16	10.63	0.20	$5.52 \times 10^{-12}$
4	28.33	0.40	$6.35 \times 10^{-12}$	4	14.16	14.16	0.27	$5.97 \times 10^{-12}$
$D_0 = 6.19 \times 10^{-12} \left( \frac{m^2}{s} \right)$				$D_0 = 6.19 \times 10^{-12} \left( \frac{m^2}{s} \right)$				

**Table 3 - Chloride ion diffusion coefficients values  $\frac{W}{C}=0.36$  and  $F_c = 56.78$  MPa**

Uniaxial stress				Biaxial stress				
Sample	$\sigma_{c(x)}$ (MPa)	$\mu_1$	Dc( $\mu_1$ ) (m <sup>2</sup> /s)	Sample	$\sigma_{c(x)}$ (MPa)	$\sigma_{c(y)}$ (MPa)	$\mu_2$ $\mu_1 = 0.3$	Dc( $\mu_1$ ) (m <sup>2</sup> /s)
1	7.08	0.12	$4.89 \times 10^{-12}$	1	14.16	3.54	0.06	$4.46 \times 10^{-12}$
2	14.16	0.25	$4.84 \times 10^{-12}$	2	14.16	7.08	0.13	$4.21 \times 10^{-12}$
3	21.24	0.37	$4.92 \times 10^{-12}$	3	14.16	10.63	0.19	$4.38 \times 10^{-12}$
4	28.33	0.50	$5.05 \times 10^{-12}$	4	14.16	14.16	0.25	$4.75 \times 10^{-12}$
$D_0 = 4.98 \times 10^{-12} \left( \frac{m^2}{s} \right)$				$D_0 = 4.98 \times 10^{-12} \left( \frac{m^2}{s} \right)$				

#### 4. Results and discussion

Based on the diffusion coefficient values provided in Tables 1, 2 and 3, Figure 3 (a, b, c) displays the distribution of chloride ion concentration at 30 mm depth as a function of corrosion initiation time and uniaxial stress levels  $\mu_1$  for various water-to-cement ratios (W/C).

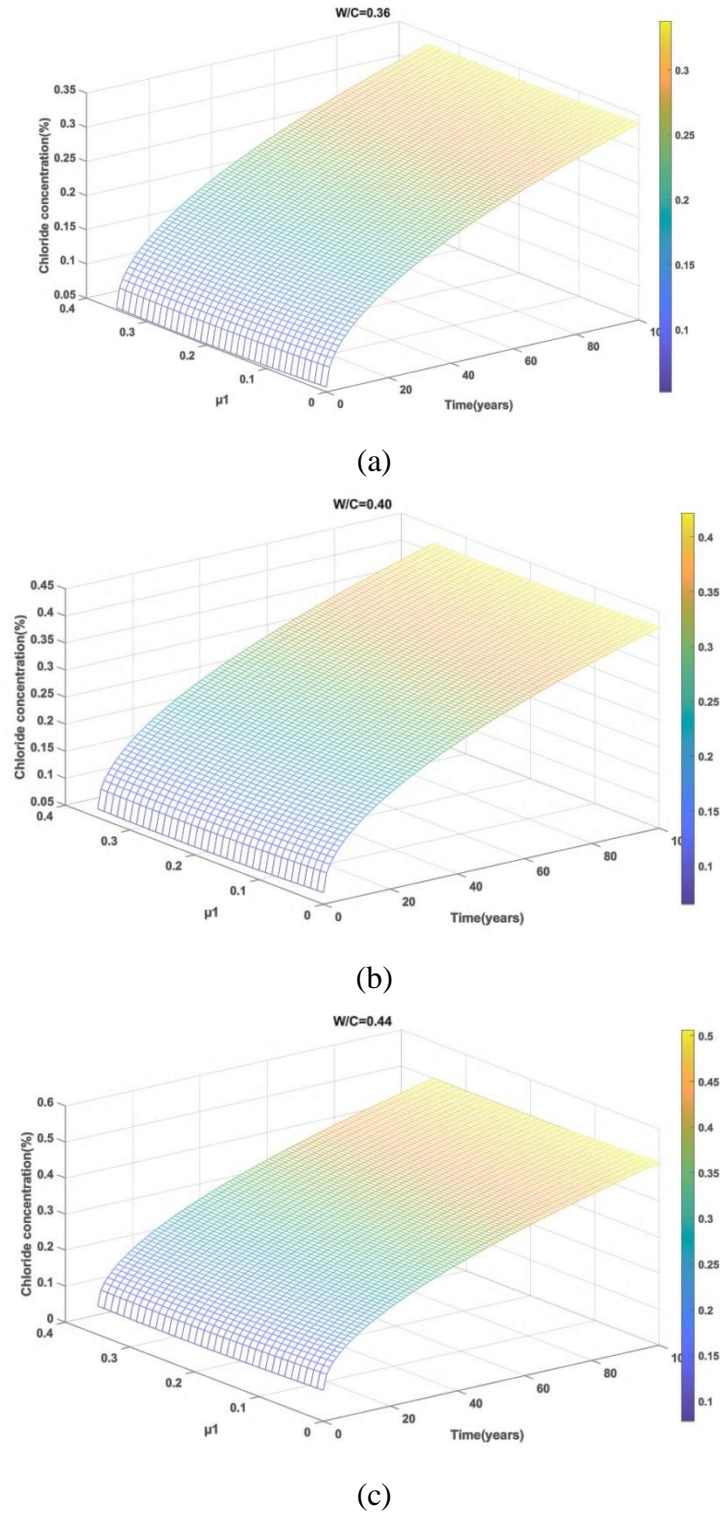
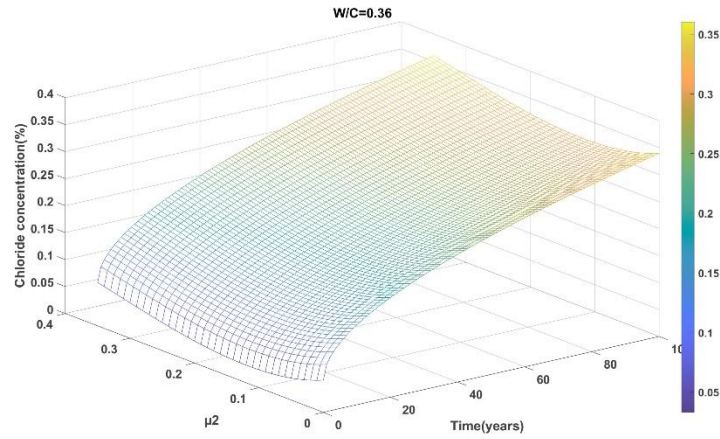
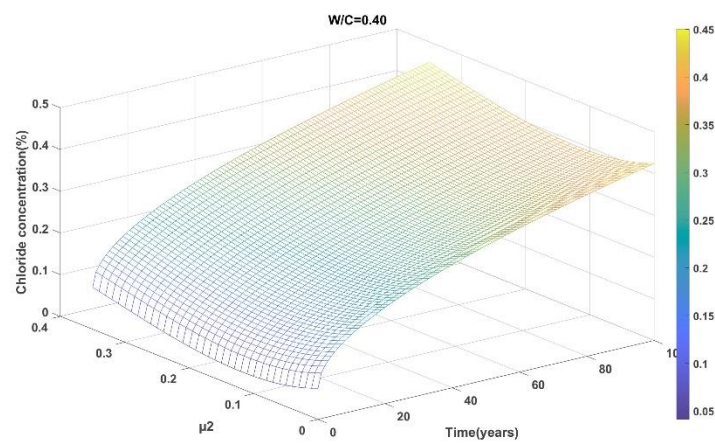


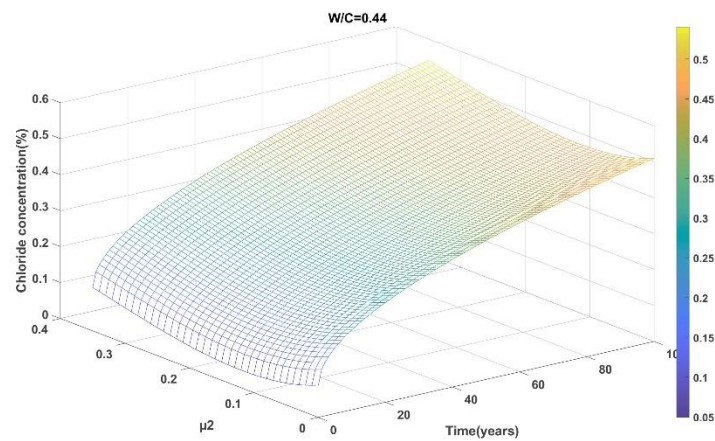
**Figure 3 - Results of chloride ion concentration distribution at a depth of 30 mm as a function of corrosion initiation time and uniaxial stress levels  $\mu_1$  for various W/C ratio**



(a)



(b)



(c)

**Figure 4 - Results of chloride ion concentration distribution as a function of corrosion initiation time with biaxial stress levels  $\mu_2$  for various W/C ratio**

We present in the following Table 4 the numerical values of concentrations as a function of the corrosion initiation time in the uniaxial and biaxial cases.

**Table 4 - Concentration values for uniaxial and biaxial cases**

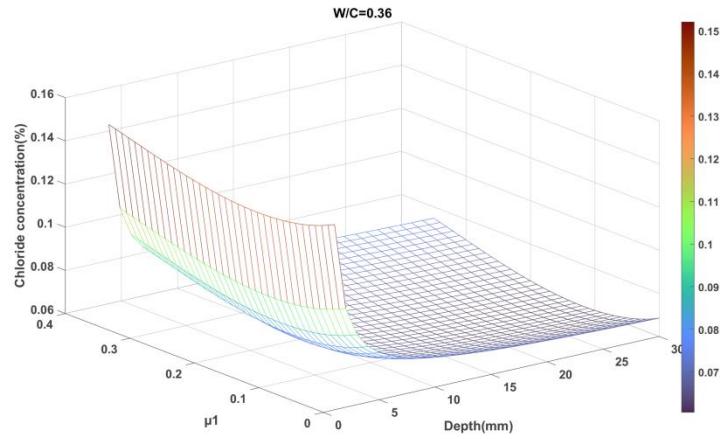
$\frac{W}{C}$	Uniaxial stress			Biaxial stress			
	Time(years)	$\mu_1$	Chloride concentration (%)	Time(years)	$\mu_2$	Chloride concentration (%)	$\mu_1$
0.44	20	0.15	0.211	20	0.07	0.202	0.30
	40	0.30	0.241	40	0.15	0.231	0.30
	60	0.45	0.270	60	0.22	0.263	0.30
	80	0.60	0.304	80	0.30	0.321	0.30
0.40	20	0.13	0.213	20	0.07	0.206	0.27
	40	0.27	0.243	40	0.13	0.234	0.27
	60	0.40	0.267	60	0.20	0.266	0.27
	80	0.54	0.289	80	0.27	0.298	0.27
0.36	20	0.12	0.222	20	0.06	0.203	0.25
	40	0.25	0.242	40	0.12	0.234	0.25
	60	0.37	0.264	60	0.19	0.262	0.25
	80	0.50	0.292	80	0.25	0.287	0.25

Considering the stress level and the age factor (aging), Figure 3(a, b, c) and the results in Table 4 show the increase in chloride ion concentration between (0.2:0.3%) as a function of corrosion initiation time at several steps (20, 40, 60, 80) years in the coating layer of aged ordinary concrete when the stress level is uniaxial for progressive W/C ratios (0.36, 0.40, and 0.44) is compatible with that proposed by Petr Lehner *et al.* [10]. Figure 4 (a, b, c) and the results in Table 4 support this finding, but only for biaxial loading. The concentration of chloride ions directly affects the corrosion initiation time of metal reinforcement in aged concrete. The higher the concentration, the faster corrosion initiation occurs at both uniaxial and biaxial stress levels.

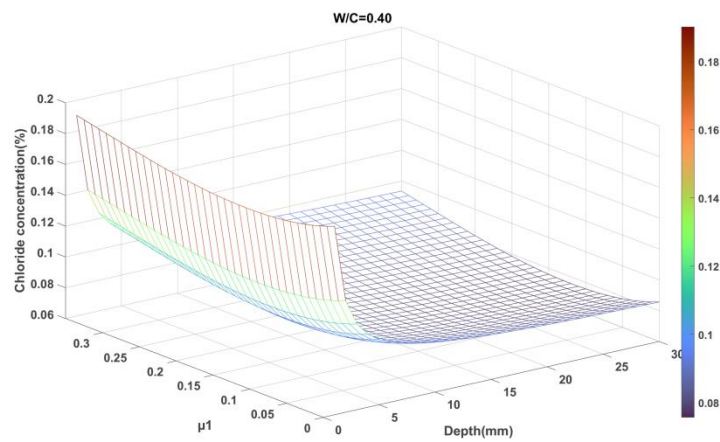
The (W/C) ratio is also an important parameter in estimating service life based on the free distribution of chloride ion concentration in aged reinforced concrete structures subjected to uniaxial and biaxial stresses caused by the acceleration of corrosion initiation time. Figures 3 and 4 show this clearly, as does Table 4.

Figure 5 (a, b, c) displays the distribution of chloride ion concentration as a function of concrete cover thickness and uniaxial stress level ( $\mu_1$ ) for three water-to-cement ratios (W/C). The stress level ( $\mu_1$ ) affects the ion concentration distribution in concrete, resulting in a decrease ranging from 0.14:0.13%. The diffusion of chloride ions in the thickness of the coating (0:30) mm for various (W/C) ratios of 0.44, 0.40, and 0.36 is consistent with the model proposed by Cheng *et al.* [5], following an exponential law until reaching the reinforcement.

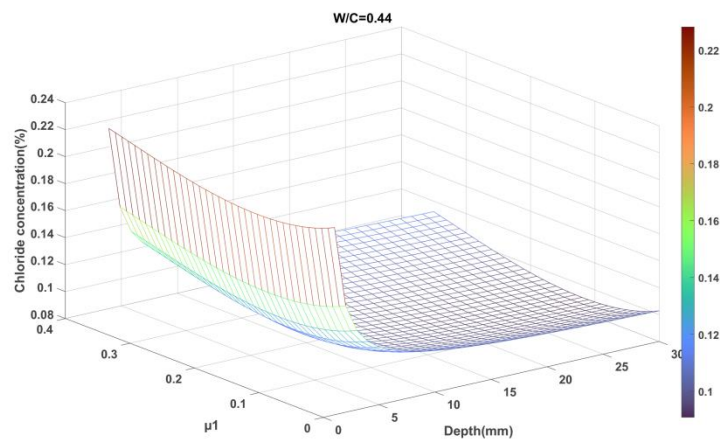




(a)



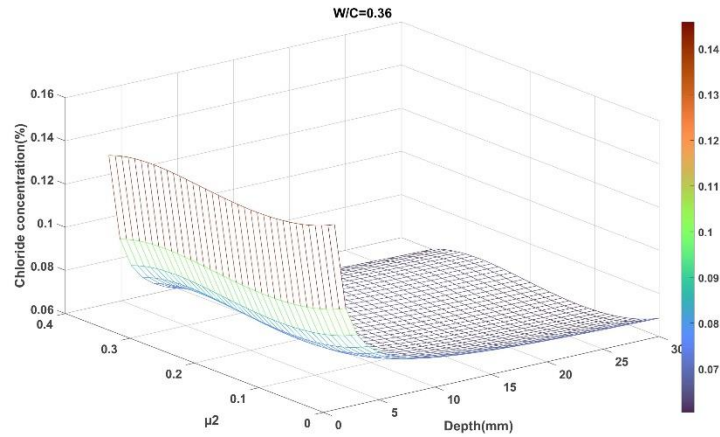
(b)



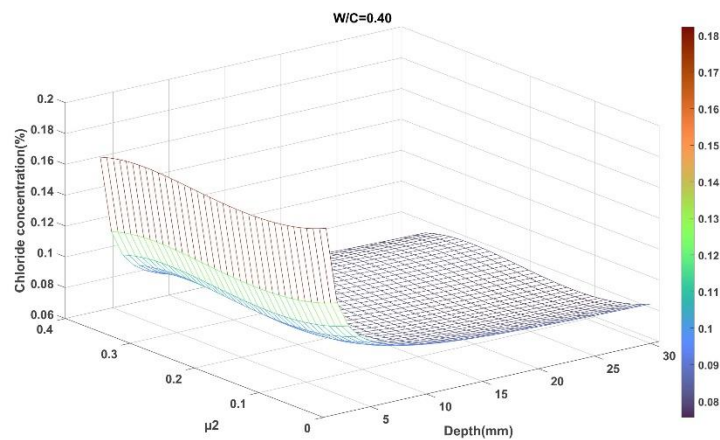
(c)

**Figure 5 - Results of chloride ion concentration distribution as a function of concrete coating thickness with uniaxial stress level  $\mu_1$  for three water-to-cement ratios (W/C).**

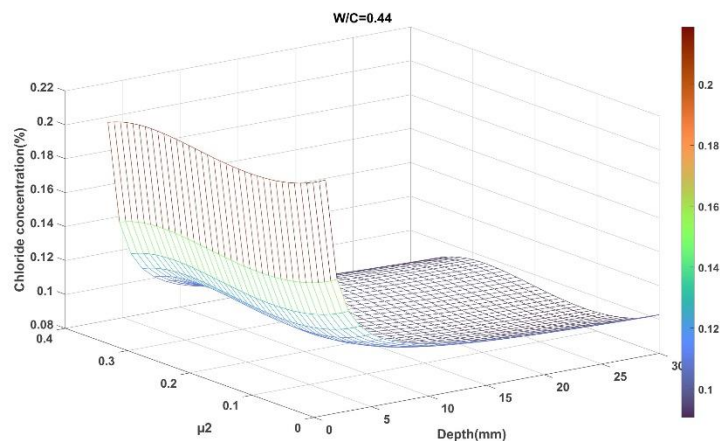
Figure 6 (a, b, c) shows the distribution of chloride ion concentration as a function of concrete coating thickness with a biaxial stress level ( $\mu_2$ ) and three water-to-cement ratios(W/C). Mechanical loading has a greater impact on ion concentration distribution when biaxial stresses are present ( $\mu_2$ ). The diffusion of chloride ions in the coating thickness (0:30) mm at various (W/C). ratios (0.44, 0.40, and 0.36) is comparable to that proposed by Cheng *et al.* [5].



(a)



(b)



(c)

**Figure 6 - Results of chloride ion concentration distribution as a function of concrete coating thickness with a biaxial stress level  $\mu_2$  for three water-to-cement ratios (W/C)**

The concentration values are displayed in Table 5. The concentration of chloride ions in the aggressive medium affects the value of the concrete coating, particularly when the aging effect is taken into account. This concentration weakens the concrete's structure and impairs its ability to protect reinforcement from corrosion, resulting in accelerated age-related deterioration of the structure. The simulation also demonstrates that increasing the (W/C) ratio has a significant impact on the free concentration distribution, indirectly increasing porosity and thus facilitating the

transport of chloride ions through the thickness of the coating of old structures by accelerating deep diffusion towards the metal reinforcement.

We present in the following Table 5 the numerical values of concentrations as a function of the coating thickness in the uniaxial and biaxial cases.

**Table 5- Concentration values**

$\frac{W}{C}$	Uniaxial stress			Biaxial stress			
	Depth(mm)	$\mu_1$	Chloride concentration (%)	Depth(mm)	$\mu_2$	Chloride concentration (%)	$\mu_1$
0.44	5	0.15	0.142	5	0.07	0.125	0.30
	10	0.30	0.137	10	0.15	0.127	0.30
	20	0.45	0.139	20	0.22	0.138	0.30
	30	0.60	0.142	30	0.30	0.163	0.30
0.40	5	0.13	0.141	5	0.07	0.124	0.27
	10	0.27	0.138	10	0.13	0.127	0.27
	20	0.40	0.136	20	0.20	0.133	0.27
	30	0.54	0.140	30	0.27	0.141	0.27
0.36	5	0.12	0.142	5	0.06	0.124	0.25
	10	0.25	0.137	10	0.12	0.128	0.25
	20	0.37	0.134	20	0.19	0.132	0.25
	30	0.50	0.139	30	0.25	0.140	0.25

## 5. Conclusion

This study aimed to build a numerical model that characterizes the response of structures to corrosion caused by chloride ion attack. Specifically, we focus on modelling the changes in the diffusion coefficient, considering the interplay between three factors: the magnitude of compressive stress, the aging factor, and the water-to-cement  $W/C$  ratio. The model accurately replicates the experimental findings documented in the literature, where each factor was examined independently. The model verifies that the infiltration rate of chloride ions escalates as the  $W/C$  ratio and stress levels, whether uniaxial or biaxial, increase. The age of the concrete influences the diffusion coefficient of chloride ions.

The findings show that older concrete allows for better propagation of ions compared to new concrete. By combining multiple parameters into a single model, we can gain a more comprehensive understanding of the individual impact of each parameter on the phenomenon, which is the primary objective of this study. Various factors in concrete affect the spread of chloride ions and, consequently, the onset of corrosion in the reinforcement. Nevertheless, this model accurately replicates the rate at which chloride ions spread and consequently affects the durability of concrete by considering three key parameters. The model can be enhanced by either extending its applicability to different types of loading or by considering additional factors that affect the corrosion of reinforcement in reinforced concrete structures, such as the occurrence of cracking.

## References

- [1] Sohail, M. G., Kahraman, R., Nasser, A. N., Gencturk, B., & Alnahhal, W. (2021). Durability characteristics of high and ultra-high performance concretes. *Journal of Building Engineering*, 33, 101669. <https://doi.org/10.1016/j.jobe.2020.101669>
- [2] Yong, D. (2020). Effect of acid rain pollution on durability of reinforced concrete structures. IOP Conference Series: Earth and Environmental Science, 2nd International Conference on Air Pollution and Environmental Engineering, Xi'an, China/450: 012115. <https://iopscience.iop.org/article/10.1088/1755-1315/450/1/012115>
- [3] Ovchinnikov, I. I., Snezhkina, O. V., & Ovchinnikov, I. G. (2020). Probabilistic assessment of the durability of reinforced concrete piles under chloride aggression. IOP Conference Series: Materials Science and Engineering, 753(1) :022072. <https://iopscience.iop.org/article/10.1088/1757-899X/753/2/022072>
- [4] Kušter Maric, M., Ožbolt, J., Balabanic, G., Zhychkovska, O., & Gambarelli, S. (2020). Chloride transport in cracked concrete subjected to wetting – drying cycles: numerical simulations and measurements on bridges exposed to de-icing salts. *Frontier in Built Environment*, 6, 561897. <https://www.frontiersin.org/articles/10.3389/fbuil.2020.561897>
- [5] Cheng, X., Peng, J., Cai, C. S., & Zhang, J. (2020). Experimental study on chloride ion diffusion in concrete under uniaxial and biaxial sustained stress. *Materials*, 13(24), 5717. <https://doi.org/10.3390/ma13245717>
- [6] Yinglong, L., Pengzhen, L., & Junjun, M. (2020). Diffusion behavior of chloride ions in concrete box girder under the influence of load and carbonation. *Materials*, 13(9), 2117. <https://doi.org/10.3390/ma13092117>
- [7] Hodhod, O. A., & Ahmed, H. I. (2014). Modeling the corrosion initiation time of slag concrete using the artificial neural network. *HBRC Journal*, 10(3), 231-234. <https://doi.org/10.1016/j.hbrcj.2013.12.002>
- [8] Bensaada, S. (2011). *Cours de corrosion*. Office des Publications Universitaires (OPU - Algérie). <https://opu.dz/fr/livre/mines-et-m%C3%A9tallurgie/cours-de-corrosion>
- [9] Ollivier, J. P., & Vichot, A. (2008). *La Durabilité des Bétons : bases scientifiques pour la formulation de bétons durables dans leur environnement*. Presses de l'école nationale des Ponts et Chaussées.
- [10] Lehner, P., & Konečný, P. (2017). Numerical validation of concrete corrosion initiation model considering crack effect model and aging effect. *Procedia Engineering*, 190, 154 – 161. <https://doi.org/10.1016/j.proeng.2017.05.321>
- [11] Zhao, X., Gao, H., Fan, W., Duan, Y., Shang, Y., & Hou, J. (2020). Design and Durability Analysis of Marine Concrete. IOP Conference Series: Earth and Environmental Science, 4th International Conference on Water Conservancy, Hydropower and Building Engineering, Lanzhou, China / 560 :012035. <https://iopscience.iop.org/article/10.1088/1755-1315/560/1/012035>
- [12] Horňáková, M., Lehner, P., Le, T.D., Konečný, P., & Katzer, J. (2020). Durability characteristics of concrete mixture based on red ceramic waste aggregate. *Sustainability*, 12(21), 8890. <https://doi.org/10.3390/su12218890>